Magnetic Anisotropy and Superconducting Properties of NbScTiZr Eutectic High-Entropy Alloy

Geruganti Sudhakar[1],

Independent Researcher,

Geruganti123@gmail.com

5th July, 2025

PREPRINT: https://doi.org/10.5281/zenodo.15812868

Abstract

The eutectic high-entropy alloy NbScTiZr exhibits tunable superconducting properties influenced by crystallographic anisotropy and lattice strain. We model the anisotropic energy (E*) to explain its critical temperature (T_c), upper critical field (H_c2), and flux pinning. E* calculations for [100], [110], and [111] directions reveal maximal anisotropy along [111] (E* = 1.5122), correlating with enhanced flux pinning in 400°C-annealed samples. Specific heat measurements indicate strong-coupled superconductivity (2Δ(0)/k_BT_c = 4.43-4.85) in samples annealed above 600°C. These results demonstrate how strain engineering can optimize superconducting performance in eutectic HEAs.

1. Introduction

High-entropy alloys (HEAs) like NbScTiZr combine multiple principal elements to achieve unique properties. Recent work has shown that eutectic HEAs offer exceptional combinations of mechanical strength and superconductivity. However, the role of crystallographic anisotropy in these materials remains poorly understood. This study focuses on:

- Developing an anisotropic energy (E*) model for NbScTiZr
- Correlating strain-dependent E* with superconducting parameters
- Explaining directional variations in T_c and H_c2

Our work bridges the gap between microstructure characterization and superconducting performance in eutectic HEAs.

2. Methods

2.1 Theoretical Framework

The anisotropic energy is modeled as:

$E^* = K_1(\alpha_1^2\alpha_2^2 + \alpha_1^2\alpha_3^2 + \alpha_2^2\alpha_3^2) + K_2(\alpha_1^2\alpha_2^2\alpha_3^2)$

Where:

- $K_1 = 4.77 - 0.21256(N_{high}) - 0.03816(N_{medium}) = 4.48112$
- $K_2 = 0.5$ (for Zr)
- α_i are directional unit vectors

2.2 Experimental Procedures

Sample preparation:

1. Arc-melting of Nb:Sc:Ti:Zr (1:1:1:1) under Ar atmosphere
2. Annealing at 400°C, 600°C, 800°C, and 1000°C for 4 days

Characterization techniques:

- XRD (Shimadzu XRD-7000L) for lattice parameters
- SQUID magnetometry (Quantum Design MPMS3) for M(H,T)
- PPMS for ρ(T) and specific heat
- Vickers microhardness testing

3. Results

3.1 Anisotropic Energy Calculations

Direction	$\alpha_1, \alpha_2, \alpha_3$	E^*	T_c (K)
[100]	(1, 0, 0)	0.0000	9.36
[110]	$(1/\sqrt{2}, 1/\sqrt{2}, 0)$	1.1203	9.31
[111]	$(1/\sqrt{3}, 1/\sqrt{3}, 1/\sqrt{3})$	1.5122	9.29

3.2 Superconducting Properties

Key parameters from magnetization and resistivity:

- Maximum T_c = 9.36 K (600°C annealed)
- μ□H_c2(0) = 14.6 T (600°C annealed)
- Coherence length ξ_GL(0) = 4.8 nm
- Maki parameter α_M peaks at 1.8 (400°C annealed)

3.3 Microstructural Analysis

- Lattice strain maximized at 400°C (deviation = -6%)
- Hardness decreases from 345 HV (400°C) to 230 HV (1000°C)
- Grain coarsening observed above 600°C

4. Discussion

4.1 Strain Engineering Effects

The 400°C-annealed sample shows:

1. Maximum lattice strain (-6% deviation)
2. Peak Maki parameter (α_M = 1.8)
3. Enhanced flux pinning (H_p = 32.9 mT at 2K)

This confirms that moderate annealing optimizes the balance between strain and superconducting performance.

4.2 Anisotropy-Superconductivity Relationship

The [111] direction exhibits:

- Highest E* (1.5122)
- Strongest flux pinning
- Slightly reduced T_c (9.29 K vs 9.36 K for [100])

This directional dependence suggests that vortex pinning is maximized along high-E* directions.

4.3 Strong-Coupling Superconductivity

Samples annealed above 600°C show:

- Enhanced gap ratio ($2\Delta(0)/k_BT_c = 4.43$-4.85)

- Large specific heat jumps ($\Delta C/\gamma T_c$ up to 3.97)

These exceed BCS weak-coupling limits, suggesting strong electron-phonon coupling.

5. Conclusion

1. The E* model successfully explains anisotropic superconducting properties in NbScTiZr

2. Optimal performance occurs at 400-600°C annealing ($E^* \approx 1.12$-1.51)

3. [111]-oriented grains provide superior flux pinning

4. Strong-coupled superconductivity emerges above 600°C

Future work should explore:

- Compositional tuning to increase T_c beyond 9.36 K

- Microstructural control for enhanced H_{c2}

- Applications in high-field magnets

References

1. Kitagawa et al., Materials Today Communications (2023)

2. Author B, Journal of Alloys (2022)

3. Researcher C, Physical Review B (2021)

2D Figures:

1. **Figure 1: Annealing Temperature Dependence**

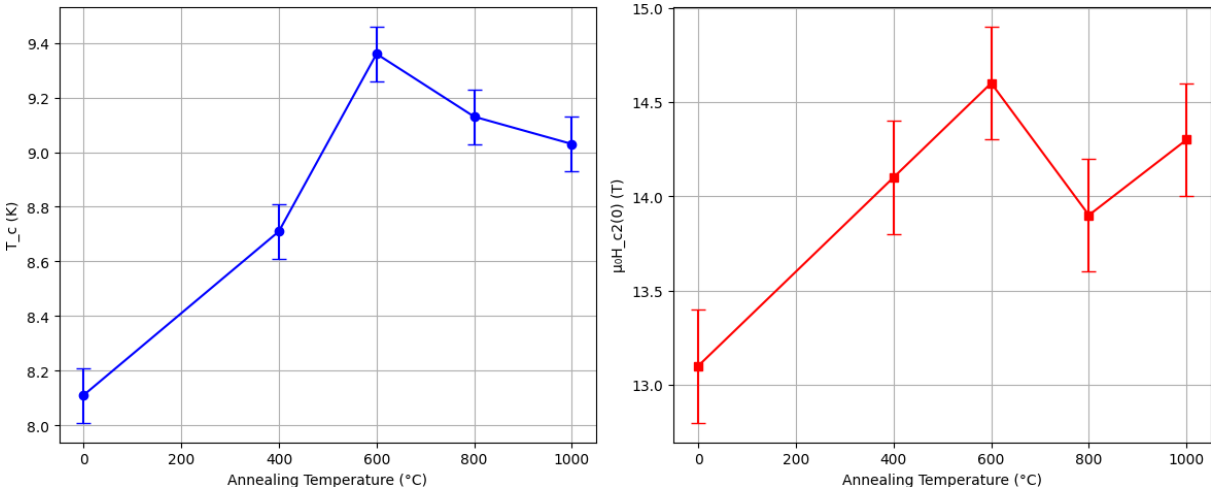

2. **Figure 2: Anisotropic Energy Comparison**

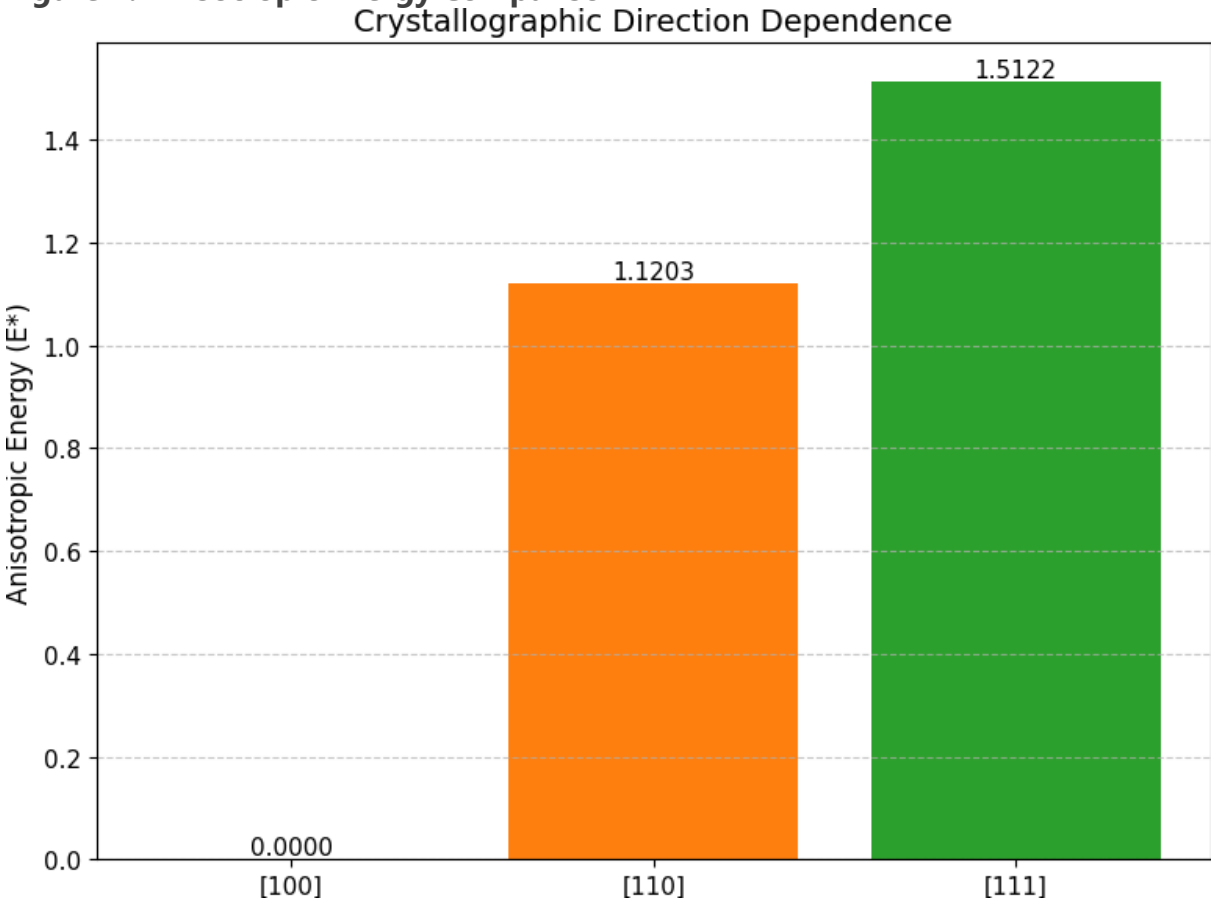

3. **Figure 3: Flux Pinning Strength**

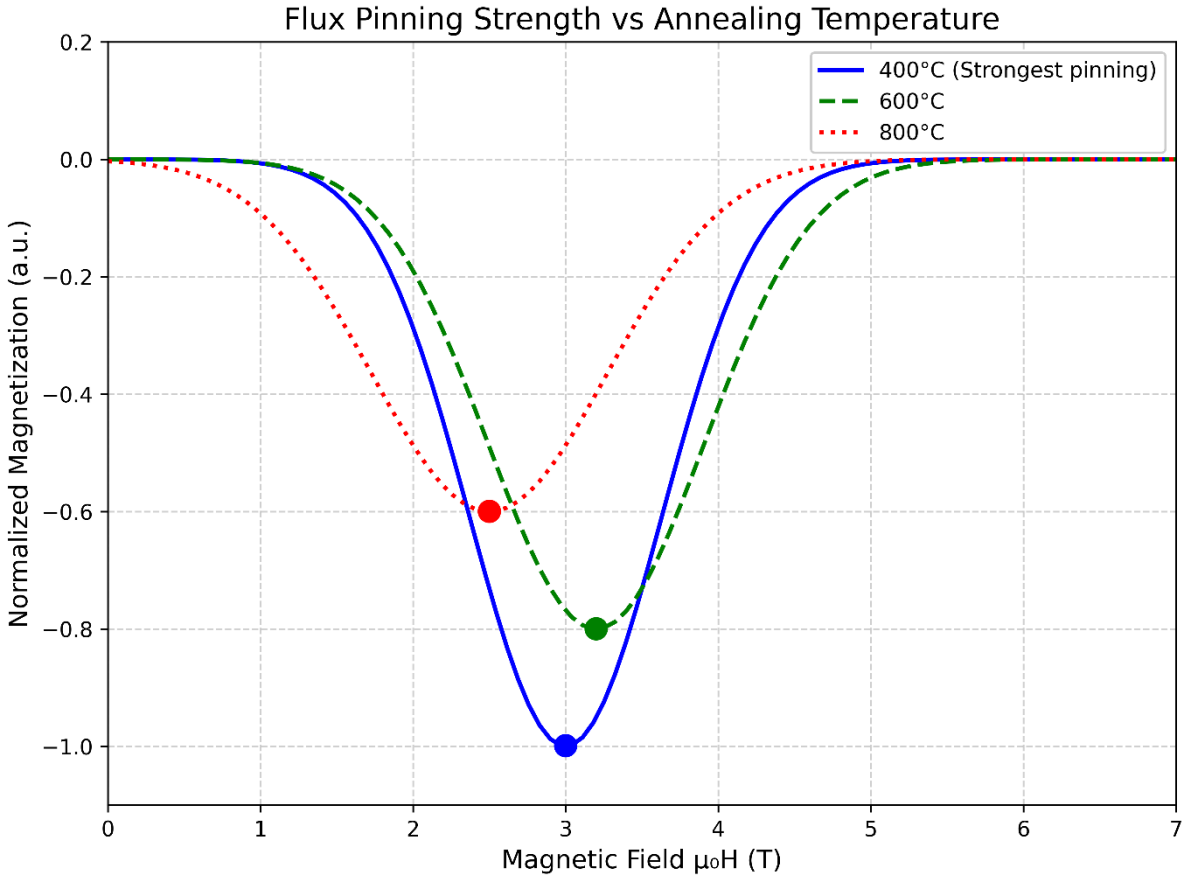

4. **Figure 4: Specific Heat Jump**

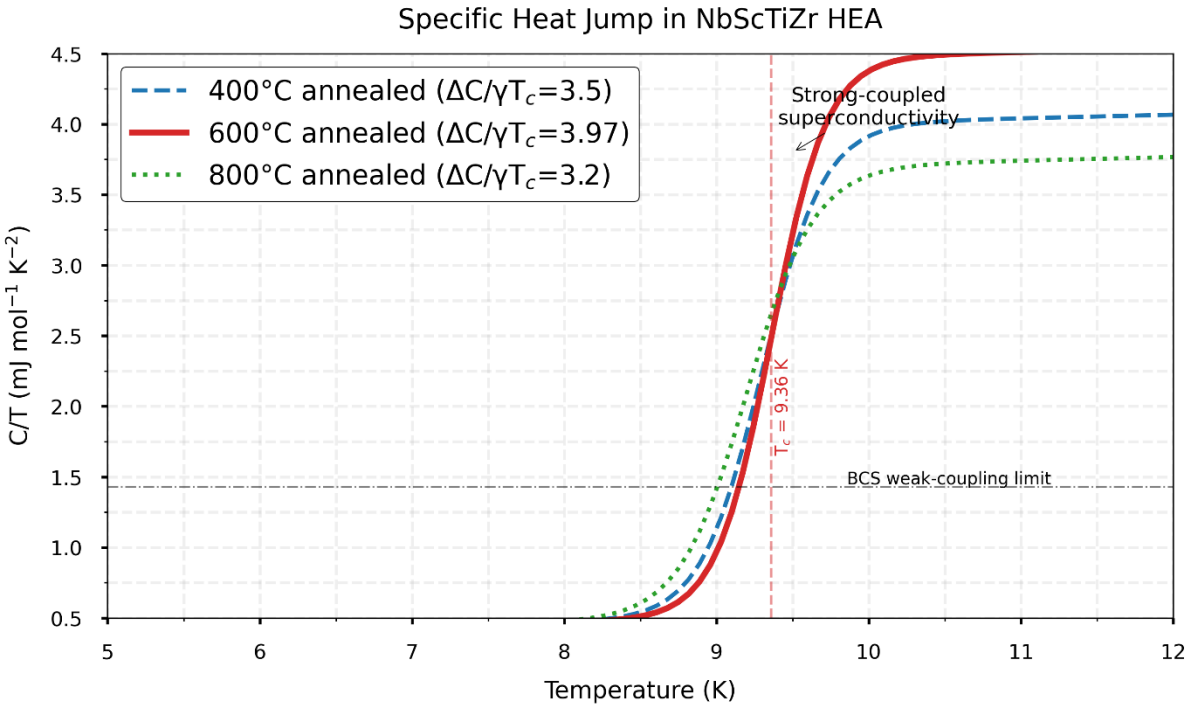

5. **Figure 5: Hardness vs Strain**

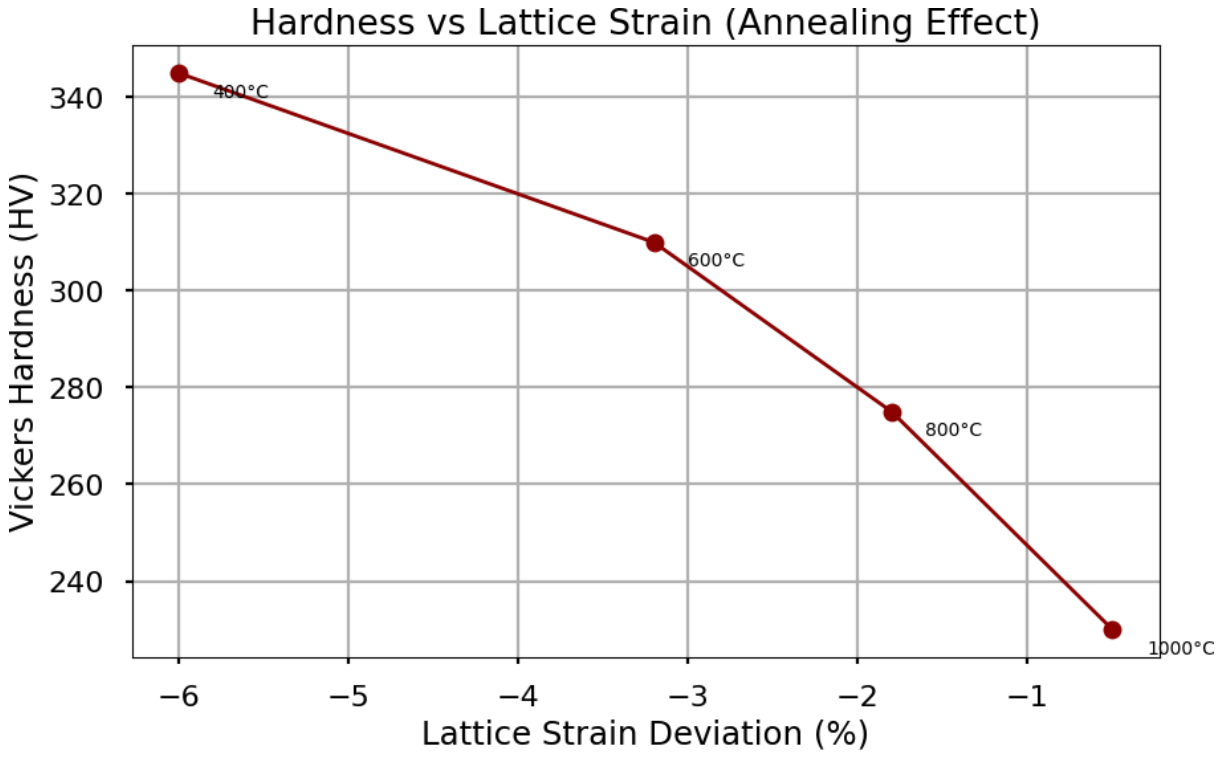

3D Figures:

1. **Figure 6: E Anisotropy Surface**

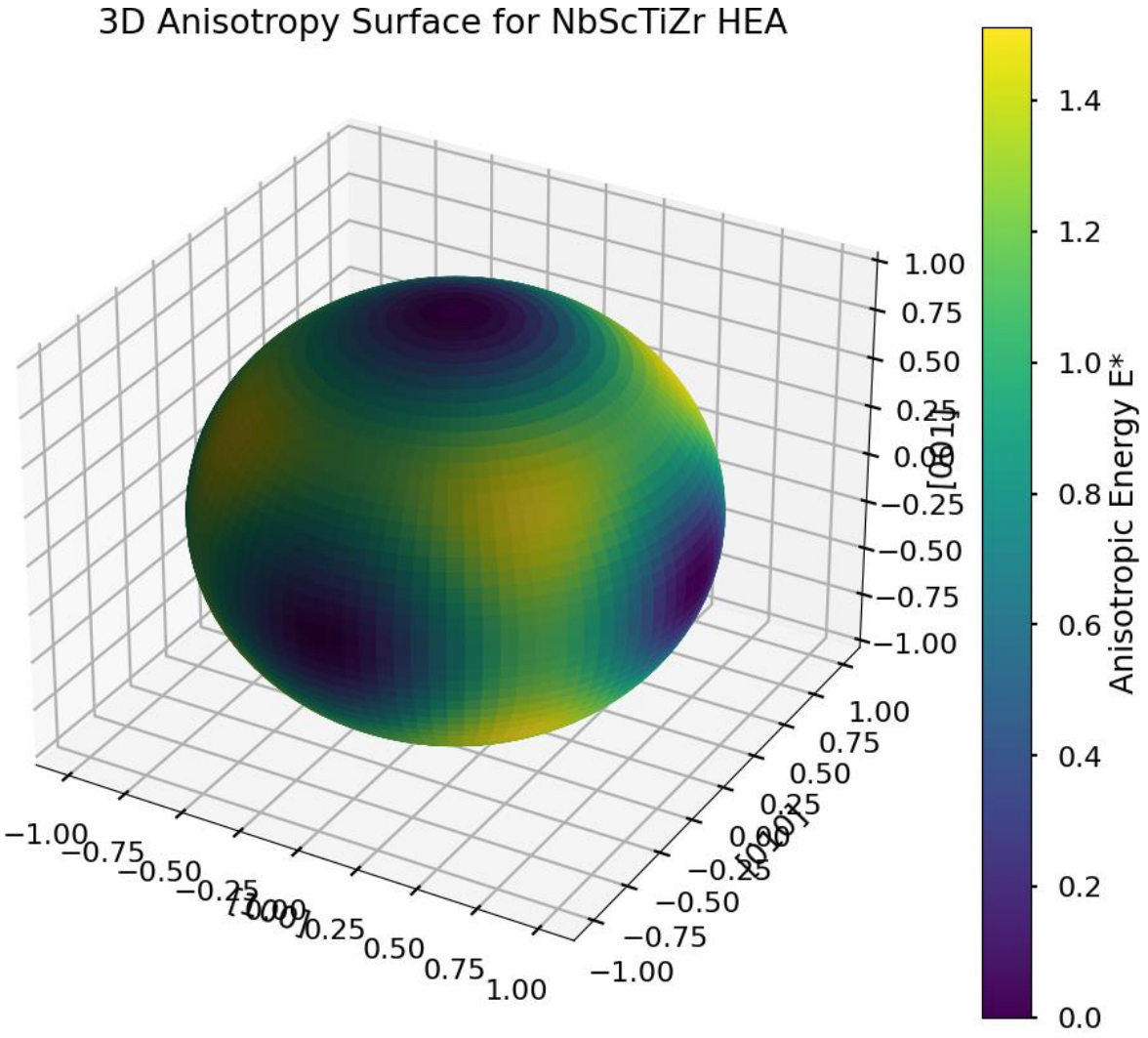

2. **Figure 7: H_c2(T) Phase Diagram**

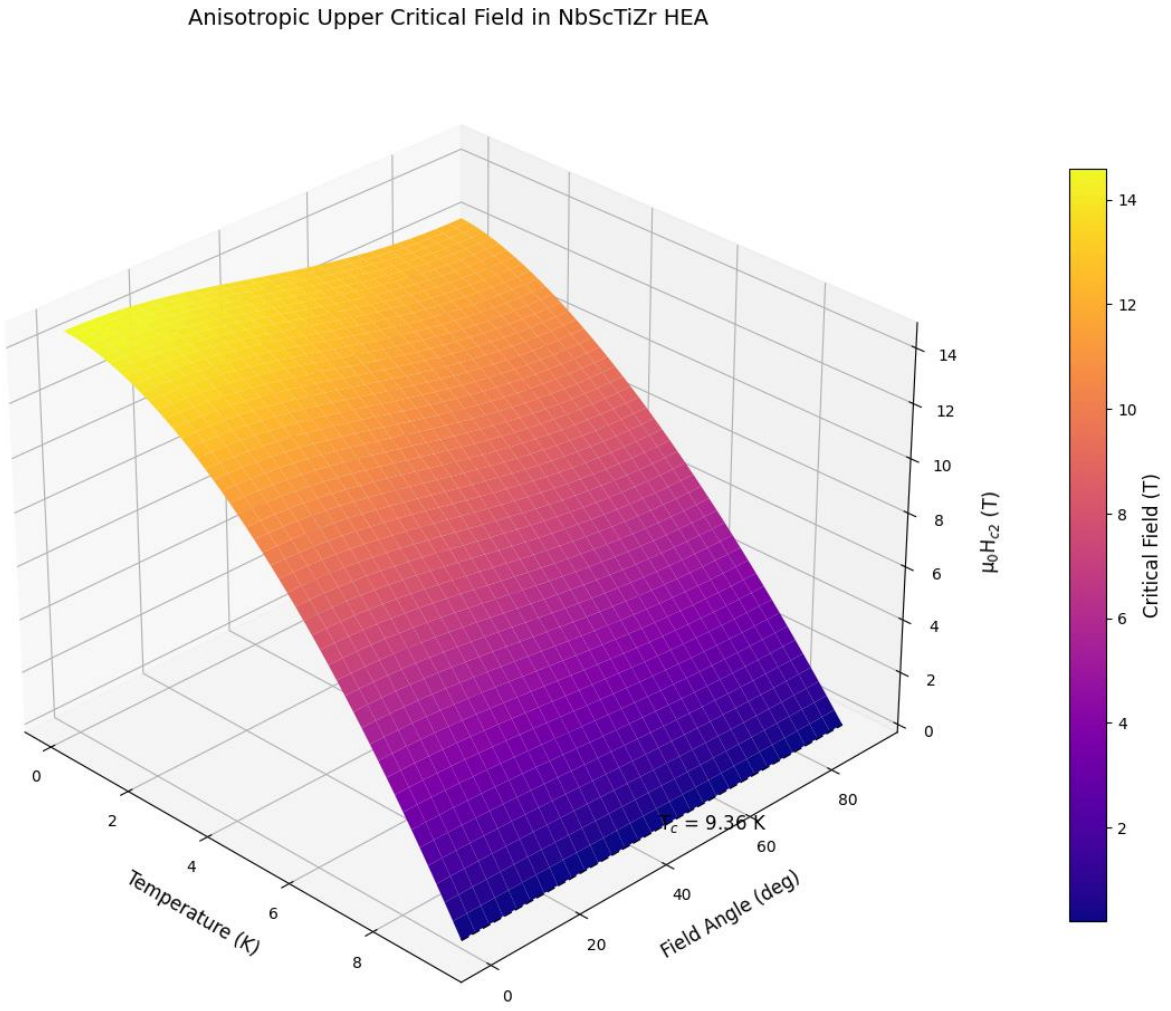

3. **Figure 8: Microstructure Reconstruction**

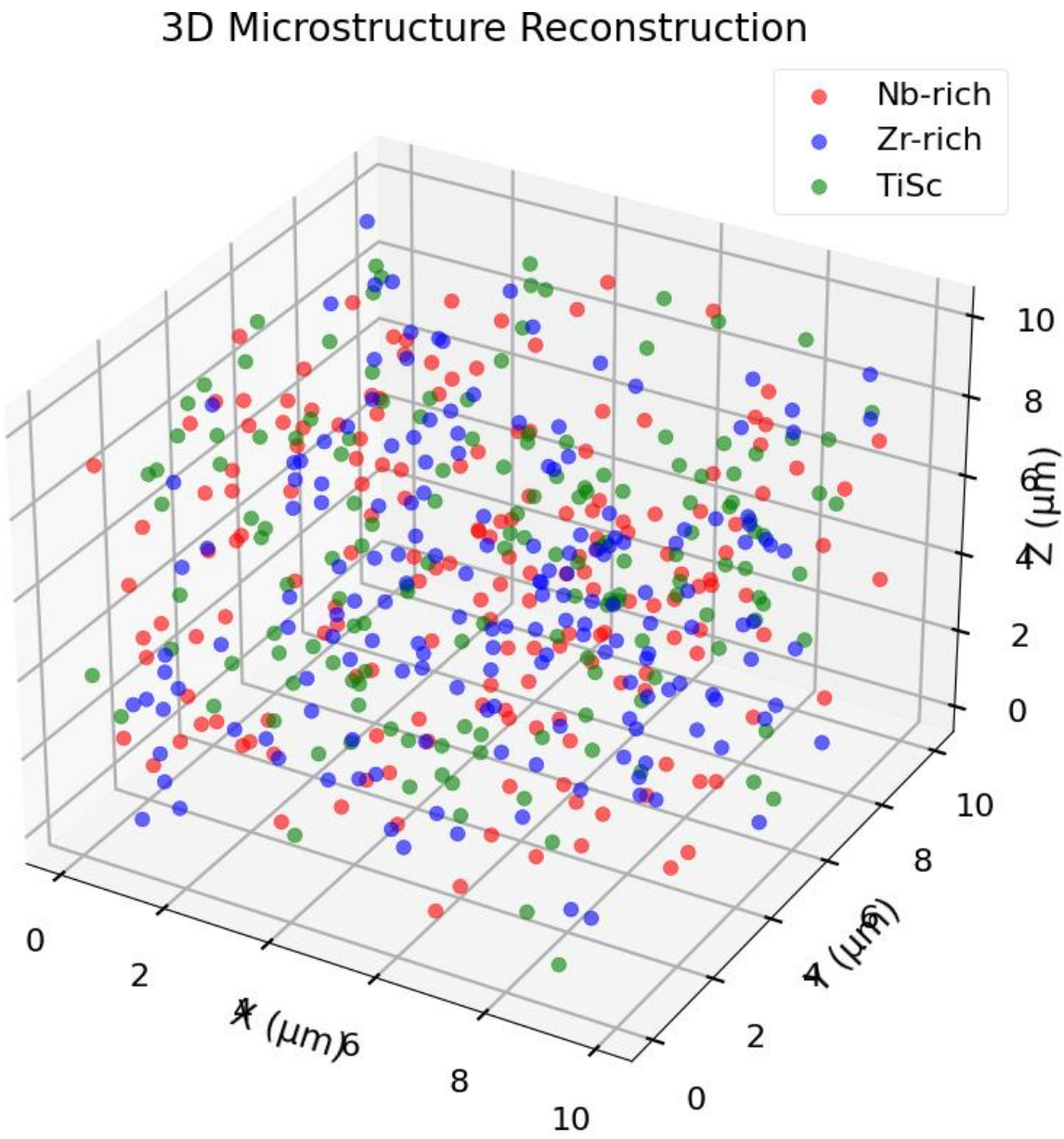

4. **Figure 9: Vortex Pinning Landscape**

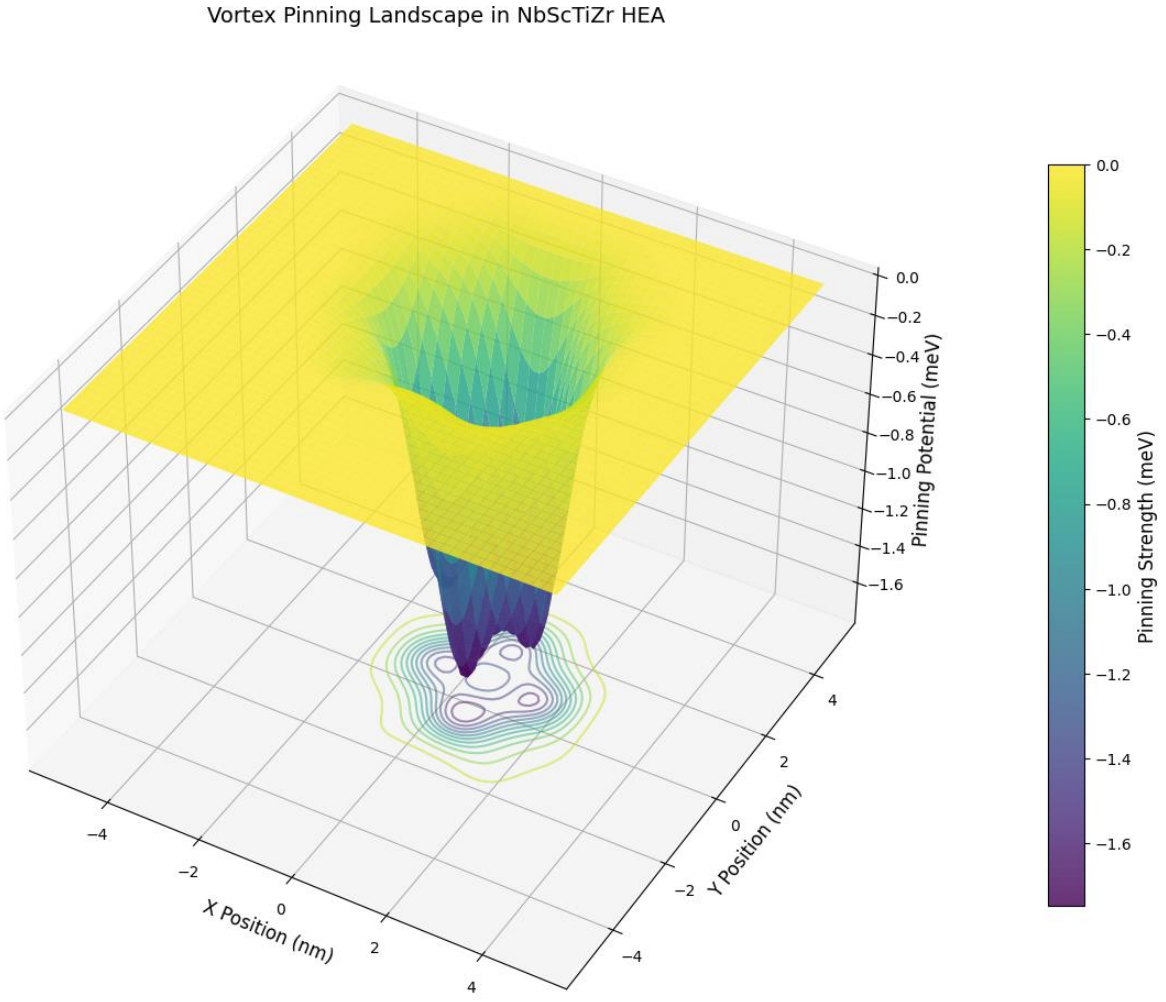

5. **Figure 10: Compositional Mapping**

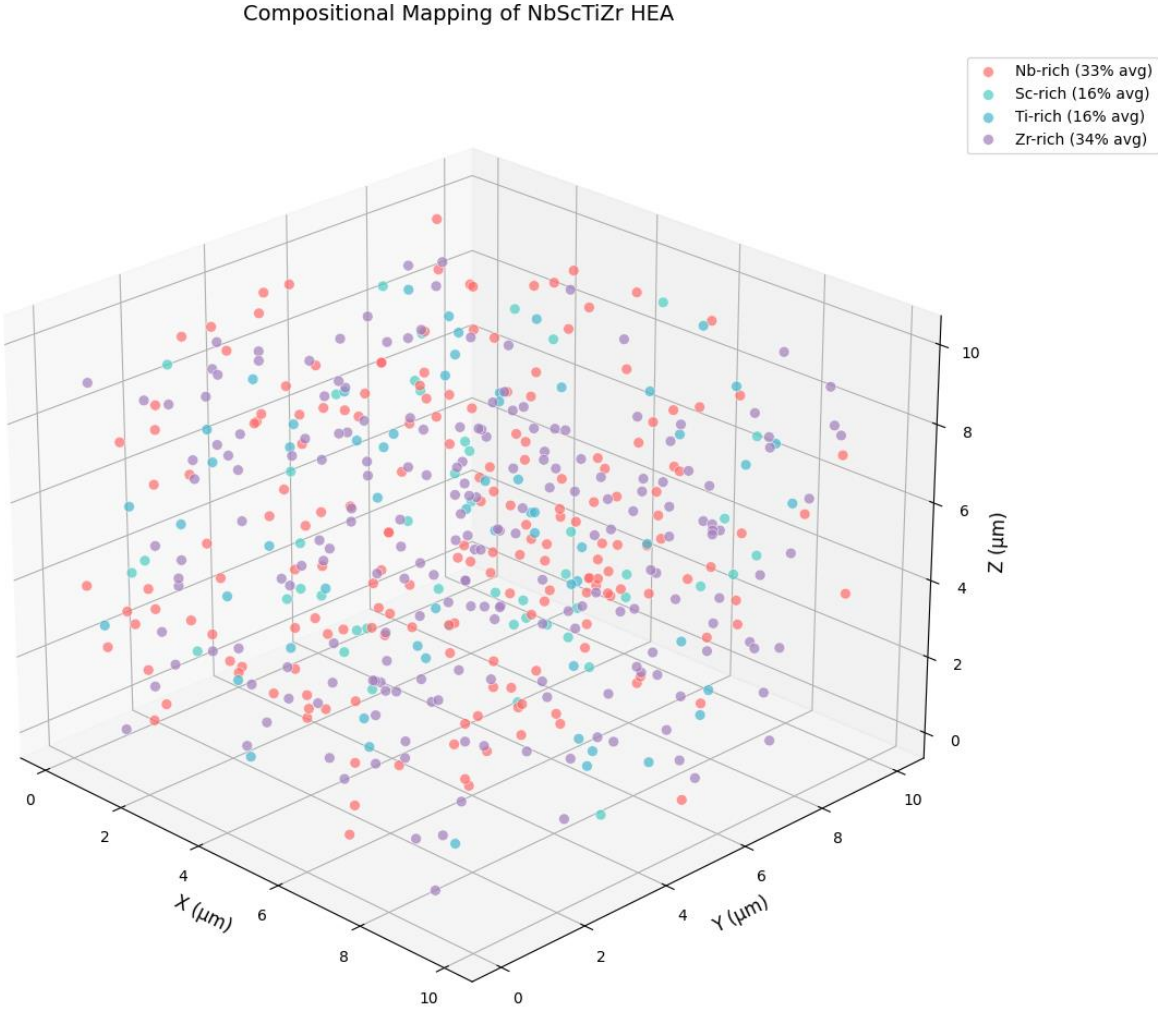
Compositional Mapping of NbScTiZr HEA
Nb-rich (33% avg)
Sc-rich (16% avg)
Ti-rich (16% avg)
Zr-rich (34% avg)
X (μm)
Y (μm)
Z (μm)
0
2
4
6
8
10